IJCB
INDONESIAN JOURNAL OF COMPUTATIONAL BIOLOGY

Research Article
Vol.1 No.1 (2022), 16-21

In Silico Study of Pertussis Toxin S1 for Recombinant Pertussis Vaccine Development in Indonesia

Ricky Rinaldi[1], Fauzian Giansyah Rohmatulloh[2], Umi Baroroh[2,3], Yusuf Sofyan Efendi[4], Mia Tria Novianti[2], Ade R.R. Firdaus[2], Toto Subroto[2,5], Muhammad Yusuf[2,5,*]

[1]Biotechnology Master Program, Postgraduate School, Universitas Padjadjaran, Bandung, West Java, Indonesia.
[2]Research Center for Molecular Biotechnology and Bioinformatics, Universitas Padjadjaran, Bandung, West Java, Indonesia.
[3]Department of Biotechnology, Indonesian School of Pharmacy, Bandung, West Java, Indonesia.
[4]PT Bio Farma (Persero), Jl. Pasteur 28, Bandung, West Java, Indonesia.
[5]Department of Chemistry, Universitas Padjadjaran, Bandung, West Java, Indonesia.

**corresponding author : m.yusuf@unpad.ac.id*

Received: July 26, 2022; **Accepted**: September 13, 2022; **Availabe Online:** September XX, 2022

Pertussis or whooping cough is a disease caused by Bordetella pertussis bacteria, and the spread disease can be controlled by vaccination. Currently, some pertussis toxoids are prepared by chemical modification, which makes it possible to change the immunospecificity. Genetic modification is considered more harmless than chemical modification to avoid altering the structure of toxoids. A mutant of R9K/E129G is known to have lower toxicity and can be used as a component of the pertussis vaccine. However, the reason behind the low toxicity of this toxoid at the molecular level remains unclear. Hence, this study aimed to investigate the molecular mechanism behind the low toxicity of R9K/E129G using molecular dynamics simulation. The structure of the mutant was built using the homology modeling approach, and the behavior of wild-type and mutant toxoid were studied by molecular dynamics simulation for 300 ns. The changes in the structure in all systems were calculated by POVME, which was further investigated by molecular docking with NAD^+ as the substrate. The results showed that the active site of the wild type was opened in the reducing environment while the mutant remained closed, which hindered the binding of NAD^+. In conclusion, the dual mutation of R9K/E129G reduces pertussis toxoid's toxicity by preventing the catalytic site's opening. Therefore, this natural mutant can be further optimized in the development of a safer vaccine for pertussis.

Keywords: Pertussis toxin | R9K/E129G mutant | molecular dynamics simulation | NAD^+ binding site | vaccine.

Bordetella pertussis bacteria are the cause behind the whooping cough and pertussis diseases. Vaccination is one of the solutions to combat this problem. In 2012, WHO reports 200,868 cases of pertussis and 95% of the cases were derived from developing countries (1). Pertussis toxin is the most important virulence factor of *B. pertussis* and is one of the targets in the process of intoxication of bacterial and genetic antigens, as well as in the ADP-ribosylation process due to the binding of NAD^+ (2). Pertussis toxin consists of an oligomer B pentameric ring and Pertussis subunit 1 (PT1) (3). PT1 is the target of detoxification in vaccine production due to the activity of ADP-ribosylation and catalyst transfer of the ADP-ribose group in the C-terminal region of GTP-binding protein (G protein) (2).

The changes in the activity of ADP-ribosyl transferase after translation become reversible and are involved in the normal cellular process. Cell signaling, DNA repair, gene regulation, and apoptosis are the changes in post-translational in cellular processes (3). Mutation in the specific PT1 residues can investigate the contribution of individual amino acid side chains in PT1 properties (4).

In the selection of a rational vaccine component, identifying the genes that encode protein pathogen is used (5). The mutation of R9K/E129G is the most recognizable mutant of pertussis toxin. Many studies have been conducted in the last 20 years, but the mechanism effect behind this mutation into the activity of pertussis toxin in the binding of NAD^+ is still unclear (6). The molecular mechanism of R9K/E129G (PT2) can be investigated by the bioinformatics approach, molecular dynamics simulation (MD) (7).

In this study, we used MD simulation to explore the behavior of wild-type and mutant of pertussis toxin. The POVME program was used to monitor the volume changes in the pocket of pertussis toxin in all systems. The molecular docking of NAD^+ and pertussis toxin was also studied to evaluate the binding of NAD^+.

Methods

Equipment

All procedures were carried out on a computer running Ubuntu 20.04.2.0 LTS and equipped with an Intel Xeon ® CPU E5-2678 v3 @2.5 GHz × 24, a GPU NVIDIA Ge Force RTX 2080Ti 6 GB, and RAMof 16 GB.

Material

The sequence of PT1 *B. pertussis* strain Pelita III was retrieved from https://www.ncbi.nlm.nih.gov, with the accession number CP019957.1(8). The structure of the *B. pertussis* Tohama 1 (PDB ID 1PRT).

Modeling of PT1 and PT2

The structure of PT1 and PT2 was constructed by homology modeling using MODELLER 9.19 (9). The sequence of PT1 *B. pertussis* strain Pelita III was retrieved from https://www.ncbi.nlm.nih.gov, with accession number

CP019957.1(8). The structure of the *B. pertussis* Tohama 1 (PDB ID 1PRT) was selected as a template for protein modeling due to the high similarity of 99.15%. The discrete-optimized protein energy (DOPE) value, statistical potential energy to evaluate the model, was used to select the best model. The model of PT1 and PT2 were evaluated by the RAMPAGE (10) program to get the results of the phi and psi torque angles in the Ramachandran plot. The model was also evaluated by the ProSA-web program to get the Z-value and determine the quality of the structure based on the similarity with the value of the experimental results (X-ray and NMR) (11,12).

Molecular Dynamics Simulation

The disulfide bridge of PT1 and PT2 was removed to mimic the endosome environment. The protonation states of histidine were adjusted using the pdb4amber provided in AmberTools 16. An explicit model system was added by a box of TIP3P water models with a minimum radius of 10Å from the surface of the protein.

All the minimization and MD simulations were performed by AMBER16 (13). In the minimization step, 1000 steps of the steepest descent algorithm were used and then 2000 steps of the conjugate gradient with 500 kcal/molÅ restraint on the backbone were applied, and the last 1000 steps of the unrestrained conjugate gradient were performed to remove any sterical clashes.

The system was gradually warmed up to stabilize at 37°C≈300 K for 60 ps in the NVT ensemble with harmonic restraint of 5 kcal/molÅ^2 on the backbone. After that, the system density and pressure were adjusted for 1000 ps in NPT. The restraint was released gradually during equilibrium to reach zero. Then the production stage is carried out for 300 ns. The timestep of the production run was 2 fs since the SHAKE algorithm was used. The Langevin thermostat was used to control the temperature and the collision frequency parameter was set to 1 ps^{-1}. The Berendsen barostat was used to control the pressure and the parameter of coupling constant and target pressure were set to 1 ps and 1 bar, respectively. The non-bonded cut-off value of 9 Å was set and Particle Mesh Ewald was activated to tread the long-range electrostatics. The MD simulation trajectory was then analyzed by AmberTools.

Binding Pockets Volume

The POVME 3.0 is used for measuring the volume of binding pocket prediction based on ligand pouches, convex gastric options, coloration, thickness and surface, and file conventions (14). The binding pockets volume was calculated at 200 to 250 ns every 10 ns from the MD simulation trajectory. The area of POVME analysis was set to 3 Å of NAD$^+$ binding site prediction of PT. Two-color boundaries were also defined as "adjacency" and "surface." Adjacency represents a thick layer of pocket volume that binds near the surface of proteins and may be interesting in measuring the burial of voxels. The surface is a thin volume layer on the surface of the protein that lines the binding pocket and is used in the calculation of surface area.

Molecular docking

AutoDock Vina was used to executing molecular docking using rigid conformations. The structure of PT1 and NAD$^+$ was docked at 240 ns from the MD simulation trajectory. The hydrogen atom was added to the polar portion to match the original environment of the molecule. The grid position of NAD$^+$ with the receptor was set to cover the whole structure. The grid set map of the ligand is then saved in the gpf format, which consists of location, position, and accurate data in the calculation. The free energy of binding from NAD$^+$ with PT1 was present as the free energy of binding (ΔG).

Results

Modeling of PT1 and PT2

The sequence of PT1 was obtained from the sequencing of *B. pertussis* Pelita III bacteria developed by PT. Biofarma for vaccine production in Indonesia (8). The template for PT1 was explored using BLAST (***https://www.ncbi.nlm.nih.gov***) and obtained the template with the PDB ID 1PRT chain A (Identity 94% and similarity 95%). Alignment sequences of PT1 and templates are presented in Figure 1. Gaps occur in the structure at positions 211 to 220 when compared to the sequence of PT1 (Figure 1).

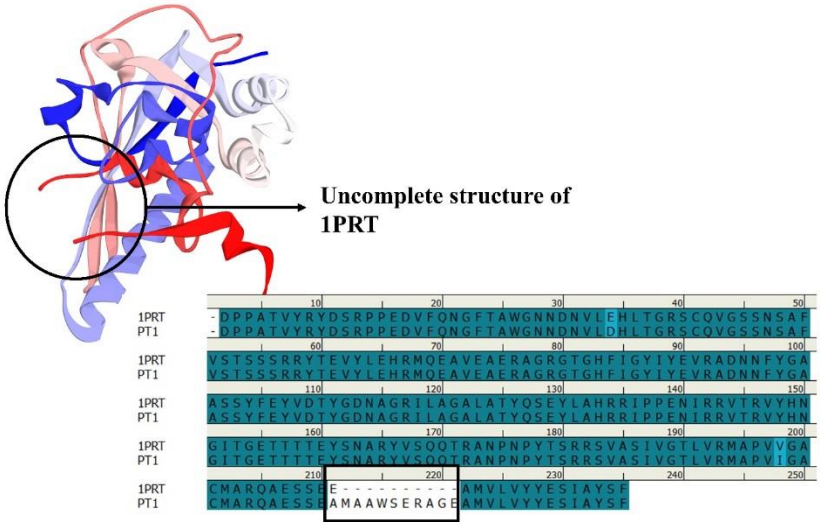

Figure 1. Crystal structure of Pertussis toxin (PDB ID 1PRT) and sequence alignment between PT1 and the template (1PRT). Uncomplete structure and gap are shown in black circle and black box, respectively.

The lowest DOPE score was chosen as a model and the quality of the model was assessed by Ramachandran plots. It is shown that 96.1% of residues were located in the most favored regions, an appropriate amount of residue in the permitted area is 3.9%, and there is no residue in the unauthorized area (Figure 2). In general, protein structures with more than 90% residue in the permitted area are categorized as a good model (15). The PROPKA (16) analysis showed that the model has a similar value to the template. The Z score value also showed a comparative score with the template, which showed -4 and -5, respectively for model and template.

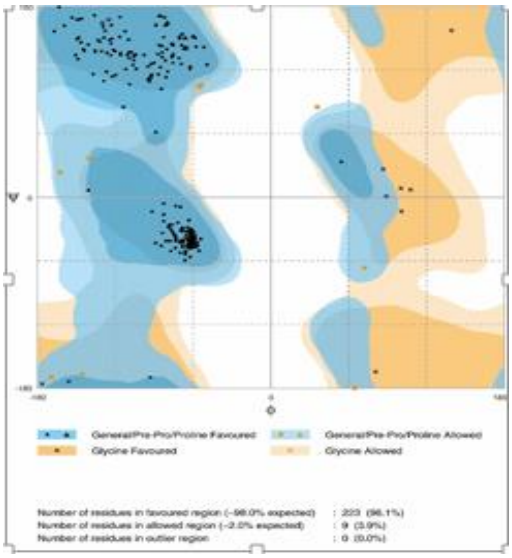

Figure 2 Ramachandran plot of PT1 model structure

Loop Stability at the Active Site Prediction (207-218) of PT1 and PT2

A 300 ns of MD simulation was performed to investigate and predict the binding site of pertussis toxin. The Root Mean Square Deviation (RMSD) of the main protein was calculated throughout 300 ns MD simulation. RMSD value represents the deviation of the receptor throughout simulation compared to the initial structure. From the graph, the changes in the structure throughout the simulation can be observed. It is shown that PT1 has a higher deviation than PT2, ± 3Å and ±2Å respectively (Figure 3). After 200 ns, the difference between PT1 and PT2 occurred. This phenomenon happened might be due to the mutation in PT2. The reason behind this finding was probably because PT1 has a loop section that frequently moves in the active site to accommodate a stable binding of NAD^+. While, in PT2 the mutations affect the shape of the loop consisting of residues 210-217 become fluctuating that PT1, hence the conformation of PT1 change to be open and make the activation pathway of the NAD^+.

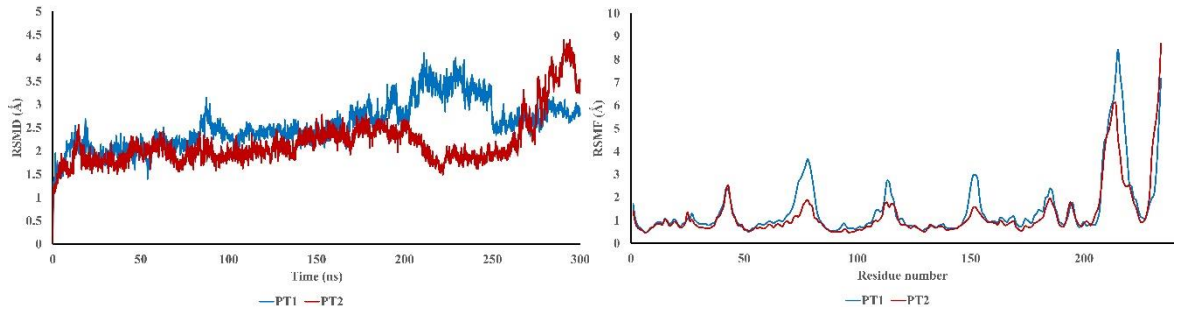

Figure 3. RMSD and RMSF profile of PT1 and PT2 throughout 300 ns of simulation**.**

The Root Mean Square Fluctuation (RMSF) plot will depict the ratio of fluctuation in a particular atom or group of atoms in the amino acid residue (17). Hence the RMSD and RMSF plots are important to carry out the prediction of structural stability on protein. The RMSF profile is shown in Figure 2, and all systems have an almost similar RMSF profile. The high fluctuation in the C-terminal, on the active site, and in several other areas is caused by the area having very high flexibility. The end of the C-terminal consists of loops that have very high flexibility, and there are no interactions that stabilize this area. High fluctuations occur at PT1 at residues number 207, 208, 210, 211, 216, 217, and 218 which are natural characters of very flexible loop structures.

Interestingly, the loop of residue number 211 to 218 opened at 240 ns in PT1 but not in PT2 (Figure 4). This loop is predicted to open the NAD^+ pathway to enter the active sites. The loop in PT1 seems more fluctuating than in PT2. This phenomenon occurs possibly because the mutant of R9K/E129G was unable to bind NAD^+ to the active site (4,16) which functions in the ADP-phosphorylation process (18), the process of cell toxification by pertussis toxin. This mutation changes the process of detoxification which can enhance the immune system through the recognition of T cells and antibodies by avoiding ADP-ribosylation and toxicity (19). From this result, the area near the loop is predicted as an active site of pertussis toxin. However, this loop at PT2 remains close throughout the simulation and it is probably the reason for the inactive of PT2.

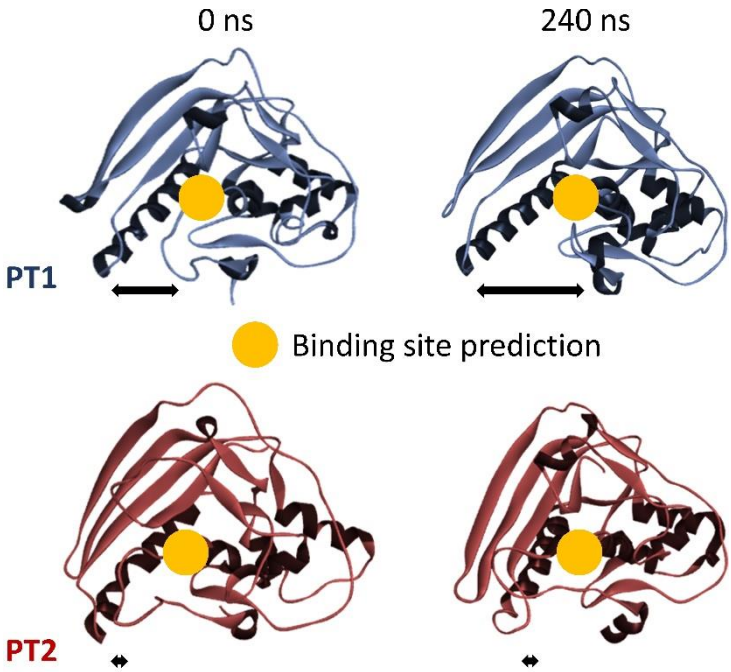

Figure 4 The snapshot of PT1 and PT2 at 0 and 240 ns. The binding site prediction and the size of loop changes are shown in orange circle and black arrow, respectively.

Binding pocket of PT1 and PT2

Both PT1 and PT2 were stable until 200 ns, hence the analysis was done after 200 ns. The binding pocket volume calculated by POVME showed that the volume has risen until 220 ns and then decrease until 250 ns (Figure 5A and 5B). The increase in volume indicated that the space of substrate, NAD^+, is sufficient. The opening of the loop around the active site made the entrance of the substrate thereby activating the ADP-phosphorylation process. Opposite of PT1, the binding pocket volume of PT2 shown fluctuating volume (Figure 6A and 6B). The size of binding volume compared to PT1 showed that the largest volume reached 5443 and PT2 1727, respectively. These sizes indicated that the larger volume of binding pocket can accommodate and provide passage for the substrate entering the active site. Differ in PT2, the size presumed that there is no path for the substrate to enter the active site and it made PT2 inactive.

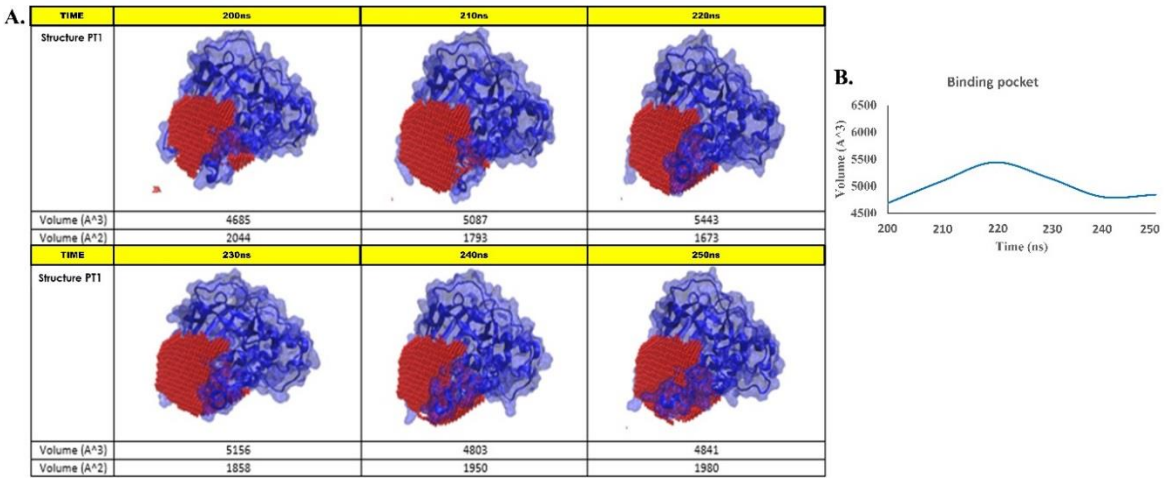

Figure 5 Volume trajectories of PT1 for 50 ns after the loop open (200 ns until 250 ns) (A) and volume diagram of the surface binding pocket (B).

A.

TIME	200ns	210ns	220ns
Structure PT2	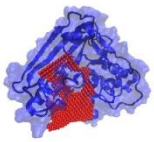	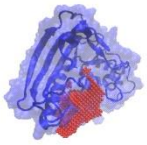	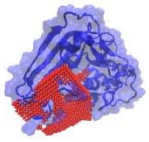
Volume (A^3)	1727	1224	1554
Volume (A^2)	1054	932	1058
TIME	**230ns**	**240ns**	**250ns**
Structure PT2	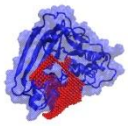	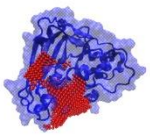	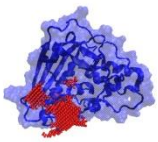
Volume (A^3)	1363	1610	1187
Volume (A^2)	1006	1106	945

B.

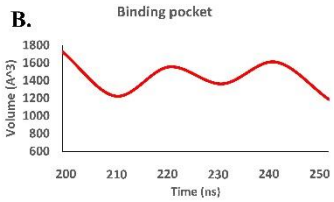

Figure 6 Volume trajectories of PT2 for 50 ns after the loop open (200 ns until 250 ns) (A) and volume diagram of the surface binding pocket (B).

The prediction of the binding pocket area of PT1 was further analyzed by molecular docking (20). The molecular docking was done at the whole structure to find the possibility of the binding pocket. After the loop at PT1 opened at 240 ns, hence this structure was used as a receptor in the docking process. The result showed that ten conformations were found in the predicted binding site. The binding affinity of NAD^+ with PT1 was -8,8 kcal/mol in the prediction binding site. In this site, NAD^+ binds to the residue Phe63, Arg66, Glu69, Hie82, Glu206, Ser207, Ala218, and Glu220 (Figure 7A and 7B). This prediction binding site is the same as finding by POVME. Hence, this site reinforces the notion that this area is an active site.

A.

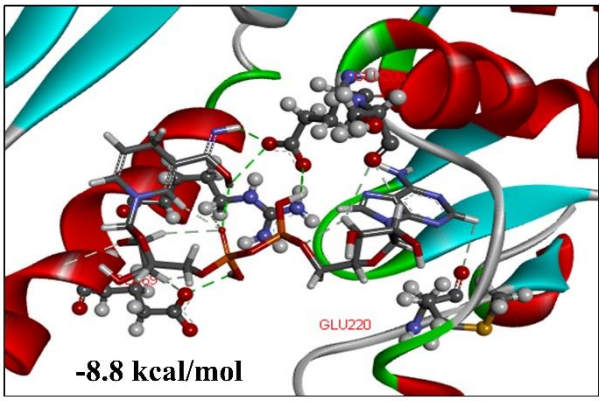

B.

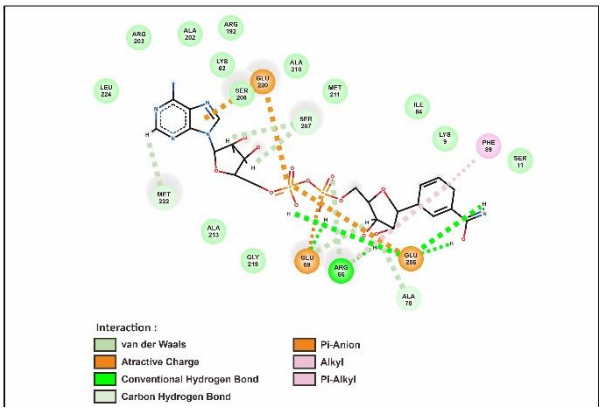

Figure 7 Molecular docking of PT1 and NAD^+ in 3D and 2D format. Hydrogen bond, attractive charge, and other molecular interaction is drawn in broken line.

Discussion

The molecular mechanism behind the low toxicity of R9K/E129G mutant toxoid is interesting to investigate. Molecular dynamics simulation is one of the comprehensive methods that can reveal the molecular mechanism at the atomic level. From the simulation, PT1 and PT2 showed differences in the loop movement at amino acid residues Ala211, Ser216, Glu217, Arg218, and Ala219 in the process of opening and closing. Predicted loop to open the NAD^+ pathway to enter the direction of the active sites that exist in the pertussis toxin. The loop in PT1 looked more active movement than the loop in PT2. This effect is possible because mutant R9K/E129G was unable to bind NAD^+ to the active site prediction which function in the ADP- phosphorylation process (18) which is the process of cell toxification by pertussis toxin. This amino acid change is a detoxification process that can enhance the immune system by being more recognized against T-cells and antibodies by avoiding the ADP-ribosylation and toxicity process (18).

Conclusion

Molecular dynamics simulation showed that the most significant and most apparent fluctuating in the PT1 is Arg217, Glu216, Ala218, Ser215, and Ala210. POVME calculation showed that the dual mutation in PT2 has a smaller volume at the active site than PT1. When the loop at PT1 opened, the volume of the binding site is increased, and it is predicted to be the path of substrate entering the active site. In contrast to PT1, the close of the loop is predicted to hinder the substrate and make PT2 inactive. Hence, one of the strategies is to reduce the size of PT1 binding site in order to develop a recombinant vaccine for pertussis.

References

1. Nataprawira HM, Ayu S, Indriyani K, Olivianto E. Pertussis in Children : Problems in Indonesia. Emerg Med. 2018;8(3).
2. Seubert A, Oro UD, Scarselli M. Genetically detoxified implications for immunization and vaccines. Expert Rev. 2014;1191–204.
3. Carbonetti NH. Pertussis toxin and adenylate cyclase toxin: key virulence factors of. Futur Microbiol. 2010;5(3):455–69.
4. Jespers L, Jenne Â, Lasters I, Collen Â. Epitope Mapping by Negative Selection of Randomized Antigen Libraries Displayed on Filamentous Phage. J Mol Biol. 1997;
5. Donati C, Rappuoli R. Reverse vaccinology in the 21st century : improvements over the original design. Ann S NEW YORK Acad Sci. 2013;1–18.
6. Ausar SF, Zhu S, Duprez J, Cohen M, Bertrand T, Steier V, et al. Genetically detoxified pertussis toxin displays near identical structure to its wild-type and exhibits robust immunogenicity. Commun Biol [Internet]. 2020;3(1):1–12. Available from: http://dx.doi.org/10.1038/s42003-020-01153-3
7. Soria-guerra RE, Nieto-gomez R, Govea-alonso DO, Rosales-mendoza S. An overview of bioinformatics tools for epitope prediction : Implications on vaccine development. J Biomed Inform. 2014;
8. Efendi YS, Susanti D, Tritama E, Pasier L, Putri GNN, Raharso S, et al. Complete Genome Sequence of Bordetella pertussis Pelita III , the Production Strain for an Indonesian Whole-Cell Pertussis Vaccine. Genome Announc. 2017;5(17):12–3.
9. Fiser A, Do RK, Sali A. Modeling of loops in protein structures. Protein Sci. 2000 Sep;9(9):1753–73.
10. Lovell SC, Davis IW, III WBA, Bakker PIW de, Word JM, Prisant MG, et al. Structure validation by C α geometry: φ,ψ and C β deviation. Proteins: Structure. Funct Genet. 2003;50(3):437–50.
11. Sippl MJ. Recognition of errors in three-dimensional structures of proteins. Proteins Struct Funct Bioinforma. 1993 Dec;17(4):355–62.
12. Wiederstein M, Sippl MJ. ProSA-web: Interactive web service for the recognition of errors in three-dimensional structures of proteins. Nucleic Acids Res. 2007;35:407–10.
13. Case DA, Cheatham III TE, Darden T, Gohlke H, Luo R, Merz Jr. KM, et al. The Amber biomolecular simulation programs. J Comput Chem. 2005 Dec;26(16):1668–88.
14. Wagner JR, Sørensen J, Hensley N, Wong C, Zhu C, Perison T, et al. POVME 3.0: Software for Mapping Binding Pocket Flexibility. J Chem Theory Comput. 2017 Sep;13(9):4584–92.
15. Lovell SC, Davis IW, Iii WBA, Bakker PIW De, Word JM, Prisant MG, et al. Structure Validation by Cα Geometry : ϕ,ψand Cβ Deviation. PROTEINS Struct Funct Genet. 2003;450(August 2002):437–50.
16. Rostkowski M, Olsson MH, Søndergaard CR, Jensen JH. Graphical analysis of pH-dependent properties of proteins predicted using PROPKA. BMC Struct Biol. 2011;11(Cc).
17. Martínez L. Automatic identification of mobile and rigid substructures in molecular dynamics simulations and fractional structural fluctuation analysis. PLoS One. 2015;10(3):1–10.
18. Mart MA, Stuart AC, Roberto S, Melo F, Andrej S. Comperative Protein Structure Modeling of Genes and Genomes. Annu Rev Biophys Biomol Struct. 2000;291–325.
19. Yuen C, Asokanathan C, Cook S, Lin N, Xing D. Effect of different detoxification procedures on the residual pertussis toxin activities in vaccines. Vaccine. 2016;
20. Fukunishi Y, Nakamura H. Prediction of ligand-binding sites of proteins by molecular docking calculation for a random ligand library. Protein Sci. 2011;20:95–106.